The Cryosphere Discuss., 4, 207–232, 2010
www.the-cryosphere-discuss.net/4/207/2010/

The Cryosphere Discussions

This discussion paper is/has been under review for the journal The Cryosphere (TC).
Please refer to the corresponding final paper in TC if available.

Degree-day modelling of the surface mass balance of Urumqi Glacier No. 1, Tian Shan, China

E. Huintjes[1], **H. Li**[2], **T. Sauter**[1], **Z. Li**[2], **and C. Schneider**[1]

[1]Department of Geography, RWTH Aachen University, Wuellnerstr. 5b,
52056 Aachen, Germany
[2]Cold and Arid Regions Environment and Engineering Research Institute, CAS,
320 Donggang West Rd., 730000 Lanzhou, China

Received: 23 February 2010 – Accepted: 1 March 2010 – Published: 3 March 2010

Correspondence to: E. Huintjes (eva.huintjes@geo.rwth-aachen.de)

Published by Copernicus Publications on behalf of the European Geosciences Union.

Abstract

A distributed temperature-index melt model including potential shortwave radiation is used to calculate annual mean surface mass balance and the spatial distribution of melt rates on the east branch of Urumqi Glacier No. 1, north-western China. The lack of continuous datasets at higher temporal resolution for various climate variables suggests the application of a degree-day model with only few required input variables. The model is calibrated for a six day period in July 2007, for which daily mass balance measurements and meteorological data are available. Based on point measurements of mass balance, parameter values are optimised running a constrained multivariable function using the simplex search method. To evaluate the model performance, annual mass balances for the period 1987/88–2004/05 are calculated using NCEP/NCAR-Reanalysis data. The modelled values fit the observed mass balance with a correlation of 0.98 and an RMSE of 332 mm w.e. Furthermore, the calculated spatial distribution of melt rates shows an improvement in small-scale variations compared to the simple degree-day approach.

1 Introduction

Most glaciers in China belong to the continental type and react much slower to the worldwide trend of increasing temperatures than more marine type glaciers in Europe, America and New Zealand (Haeberli, 2003). Nevertheless, the increase of average air temperature by 0.7 °C from 1987 to 2000 in north-western China leads to significant glacial mass losses and a widespread increase in glacial meltwater and runoff (Zhang et al., 2006b).

Especially in western China and the eastern Tian Shan, glacier change is scarcely documented and climate observations in the mountainous regions are rare. Urumqi Glacier No. 1 is the best observed glacier in this region but there is still a lack of continuous datasets for various climate variables. This suggests the application of

TCD

4, 207–232, 2010

Degree-day modelling of the surface mass balance, Tian Shan

E. Huintjes et al.

a temperature-index approach for modelling glacier surface mass balance. The surrounding mountain terrain and the orientation of the glacier tongue lead to the assumption, that incoming global radiation, as one of the primary sources of heat for melt (Ohmura, 2001), plays an important role in temperature-index melt modelling for Glacier No. 1, allowing for spatially variable melt estimates (Hock, 2003). In this paper, a method of enhancing a temperature-index-based mass balance model through a radiation term is presented for Urumqi Glacier No. 1. Calculated annual mean mass balances are contrasted with the measurements. Furthermore, the spatial distribution of melt rates is compared with the simple degree-day approach and the mass balance maps published by the World Glacier Monitoring Service (WGMS).

2 Study site

Urumqi Glacier No. 1 (UG1) (43°05′ N, 86°49′ E) is located in the headwaters of the Urumqi river in the northern mid-part of the Chinese Tian Shan (Fig. 1). Among Chinese glaciers it provides the longest glaciological and climatological monitoring record, implemented by Tianshan Glaciological Station (TGS) in 1958 (Jing et al., 2006). The glacier's elevation ranges from 3.740 to 4.486 m a.s.l. and in 2005 the glacier covered an area of 1.8 km^2 (WGMS, 2007). In 1993 it divided into an east branch (~1.1 km^2) and a west branch (~0.7 km^2) and since 1988 glaciological measurements are carried out for both branches separately (Jing et al., 2006; Wang et al., 2007; WGMS, 2007). The region is one of the most continental areas of the world, influenced by polar and continental air masses from the Arctic and central Asia from autumn to spring. During the summer months monsoonal air masses account for 66 to 72% of the annual total precipitation amount (Hagg, 2003; Wang et al., 2007). Therefore, accumulation and ablation take part simultaneously in summer as large parts of the precipitation amounts are formed by snow in higher elevations.

Thus, UG1 belongs to the "summer-accumulation type" according to Ageta and Fujita (1996). During the winter months the region is dominated by continental air masses causing very low temperatures and little precipitation (Domrös and Peng, 1988; Zhang and Lin, 1992). The mean annual air temperature (1958–2003) at Daxigou Meteorological Station (Fig. 1, see also Sect. 3.1) is −5.1 °C, with a mean annual precipitation amount of 450 mm (Jing et al., 2006; Ye et al., 2005). Monthly precipitation varies from 2 to 15 mm during winter (October–March) to 118 mm in July (Jing et al., 2006). For the last climatological normal period, the mean annual temperature amplitude is 20.5 K (Hagg, 2003).The arid climate causes very large evaporation at the glacier surface so that the effect of sublimation is one of the dominant ablation processes (Zhang et al., 2006a).

3 Data

3.1 Meteorological data

At UG1 the nearest long-term meteorological record is provided by Daxigou Meteorological Station (3.540 m a.s.l., Daxigou MS) roughly 2 km east of UG1 (Fig. 1). Daxigou MS is operated by the Xinjiang Bureau of Meteorology since 1958, continuous time series of diurnal temperature and precipitation records are available from 2004, monthly means are available from 1958.

Since April 2007, the Chinese Academy of Sciences operates an automatic weather station (AWS UG1) at 4.048 m a.s.l. in the accumulation area of the east branch of UG1. Unfortunately, this AWS shows extended data gaps. A comparison of the air temperature record (April–June 2007) from this AWS with the corresponding record of Daxigou MS results in a temperature lapse rate of −0.71 K $(100\,\text{m})^{-1}$. The determination of a precipitation gradient from the available records was not possible, due to data gaps in both records and effects like snow drift and evaporation causing erroneous measurements. The calibration of the radiation module is based on hourly means of incoming shortwave radiation, measured at the AWS UG1.

TCD
4, 207–232, 2010

3.2 Mass balance data

At UG1 glacier monitoring started in 1958, with gaps between 1966 and 1976. Since then, the Chinese Academy of Sciences measures monthly mass balances using the glaciological method and calculates annual net mass balances that are published through the database of the World Glacier Monitoring Service (WGMS). Since 1988 annual net mass balances are calculated for east and west branch separately.

During a field campaign in July 2007 a dataset of daily individual stake measurements on the east branch of UG1 was compiled for calibrating a degree-day model. The dataset contains a total of 222 readings at 16 to 20 individual ablation stakes for the period from 8 to 25 July 2007. The first six days of measurements were affected by precipitation events in the evening hours, which could not be accurately captured by the weather stations. Four ablation stakes fell down in July due to strong melt. Therefore, a total of 102 readings at 16 ablation stakes during six consecutive days were selected for calibration.

3.3 Digital elevation model

Modelling of incoming shortwave radiation and surface mass balance of UG1 was based on a digital elevation model (DEM) from the Shuttle Radar Topography Mission (SRTM) database at 90 m resolution covering the glacier area and the surrounding topography. The DEM was resampled to the resolution of a LANDSAT-5 satellite image of identical coverage from 1999 (28.5 m) (Fig. 1). The glacier mask was cut out from the DEM using the boundaries determined from the LANDSAT image.

4 Model description

Simple degree-day temperature-index melt models (DDMs) have been widely applied in a variety of studies (e.g. Braithwaite, 1984; Jóhannesson et al., 1995; Zhang et al., 2006b) where sparse data is available, as they calculate melt rates based on air

TCD
4, 207–232, 2010

Degree-day modelling of the surface mass balance, Tian Shan

E. Huintjes et al.

temperature as sole measured input variable. Only restricted spatial resolution of the simulated melt rates across the glacier, induced through changes in elevation associated with the air-temperature lapse rate, can be incorporated in the model.

In order to assess more realistic spatial melt-rate variations, the relative simplicity of temperature-index models is combined with a term accounting for incoming direct shortwave radiation. The simple temperature based DDM is enhanced through the radiation term $\left(a+b\left(r/\bar{r}\right)\right)$ in an additive way (Eq. 1). The applied radiation module after Kumar et al. (1997) calculates clear sky incoming direct, diffuse and reflected shortwave radiation in response to altitude, elevation, surface gradient, orientation and position relative to neighbouring surfaces.

The first approach of an enhanced temperature-index melt model was developed by Hock (1999) and has been applied in many studies on distributed mass balance modelling (e.g. Pellicciotti et al., 2005; Schuler et al., 2005). Net shortwave radiation is the dominant source of melt energy on most glaciers (Braithwaite, 1995; Oerlemans, 2001), and thus exerts a strong influence upon the spatial evolution of melt rates due to the effects of topography. In this study, glacier melt rate M is computed by

$$M = \begin{cases} \mathrm{DDF}_{\mathrm{snow/ice}} T + \left(a+b\left(r/\bar{r}\right)\right) & T > T_T \\ 0 & T \le T_T \end{cases} \tag{1}$$

where DDF is the degree-day factor (mm K^{-1} d^{-1}), different for snow and ice surfaces, T is daily mean air temperature (°C), T_T is a threshold temperature (°C) beyond which melt is assumed to occur, a and b are radiation factors. Parameter r is daily mean estimated shortwave radiation at each grid cell of the glacier and $\bar{r}$ is daily mean shortwave radiation over all grid cells of the glacier surface (Wm^{-2}). The radiation factors are empirical coefficients which are assumed to be constant in space and time. Parameters r and $\bar{r}$ are approximated by standard algorithms on insolation geometry and topography after Kumar et al. (1997). Air temperature is extrapolated to each grid cell applying a constant lapse rate derived from air temperature data at Daxigou MS and at AWS UG1.

Accumulation is computed from precipitation measured at Daxigou MS. The precipitation amount is assumed to be constant with increasing elevation. The fraction of solid precipitation is described by a hyperbolic tangens function, depending on air temperature. The threshold is scaled within a range between 100% (0 °C) and 0% (2 °C), as suggested by Hantel et al. (2000).

The term accounting for shortwave radiation is of linear character as the result of a linear relationship of standardised shortwave radiation and the difference of measured and modelled mass balance at individual stakes (Fig. 2). Through the additive composition, the terms dependent on temperature and radiation are independent from each other as it is implied from a consideration of the energy balance (Ohmura, 2001).

5 Parameter calibration

In the radiation module after Kumar et al. (1997) the only variable factor is surface albedo, whereas the atmospheric transmission is calculated considering Rayleigh and Mie scattering as well as the absorption by atmospheric gases. For calibrating the albedo of the glacier surface, modelled mean hourly shortwave radiation that reaches the grid cell of the AWS on UG1 for a selected day during the calibration period in July 2007 is adjusted to measured mean hourly incoming shortwave radiation at the AWS at the same day. As the radiation module cannot account for the effect of clouds, a clear sky day (20 July 2007) was chosen for calibration. Albedo values were varied manually within reasonable limits until the residuals of model output and observations were minimal (Fig. 3) and the daily radiation cycle was reproduced in a satisfactory way (Fig. 4).

For UG1 the degree-day factor for ice surfaces (DDF^*_{ice}) and the radiation factors *a* and *b* are the only parameters available for calibration. Their values are adjusted such that model results are in optimal agreement with the measurements at individual stakes (Table 1). The degree-day factor for snow surfaces is assumed to be half of DDF^*_{ice} (Braithwaite and Zhang, 2000). A dataset of six consecutive days in July 2007 is used to calibrate the model parameters, whereas one mean value for each of the 16 stakes is considered. The evaluation of the model performance is conducted using a dataset of annual mean mass balances of the east branch of UG1 covering the period 1987–2005 to control whether the overall behaviour and the temporal evolution of mass balance are reproduced correctly.

Parameters are optimised running a constrained multivariable function using the simplex search method (Nelder and Mead, 1965). The parameter values were varied in an iterative process, until the residuals of model output and observations became minimal (Fig. 5). The variation of DDF^*_{ice} was restricted within reasonable limits.

Model output is produced in daily time-steps for the grid cells of individual stakes to correspond to the measurements. The optimised parameter values for the east branch of UG1 are presented in Table 1. These parameters require a site-specific calibration to avoid large errors in model values, since temperature-index melt models sensitively react to changes in degree-day factors and temperature lapse rate (Schuler et al., 2005).

In order to compare the spatial distribution of calculated melt rates produced by enhanced temperature-radiation and simple temperature based DDM, optimisation and evaluation of the simple DDM are conducted in a similar way as aforementioned, applying identical datasets and model assumptions. DDF_{ice} is the only parameter available for calibration (Table 1).

6 Results

The radiation module is calibrated by varying the albedo until the daily circles of modelled and measured incoming shortwave radiation are in optimal agreement. The manual adjustment results in an albedo value of 0.8 for the glacier surface. Comparing of measured and calculated hourly mean values for 20 July 2007 shows a correlation of 0.98, and an RMSE of 60 W/m^2 (Fig. 3). As the surrounding topography effects the incoming radiation at some glacier grid cells due to reflection or absorption, an albedo of 0.2 is attributed to the non-glaciated areas of the DEM.

On examination of the daily radiation cycles (Fig. 4), it is visible, that measured incoming shortwave radiation is overestimated during the morning hours, slightly underestimated during noon and early afternoon and again overestimated in the evening. These differences can be caused by the imprecision of the grid cells of the DEM caused by the resampling process and by differences between the actual location of AWS UG1 and the spatial mean over the whole grid cell.

For the calibration period of six days from 20–25 July 2007, a total of 102 mass balance values were derived from individual stake measurements. For each ablation stake, the measurements were merged to a single mean value. The comparison of measured and calculated values shows a correlation of 0.9, with an RMSE of 12 mm w.e. for the enhanced temperature-radiation DDM (Fig. 5).

In order to evaluate the model performance, mean net mass balance time series of the east branch of UG1 from 1987/88–2004/05 are compared to the corresponding model values (Fig. 6). Due to missing continuous meteorological records, daily temperature and precipitation data from the NCEP/NCAR-Reanalysis Project (Kalnay et al., 1996) is taken as input data. After a statistical downscaling of four NCEP/NCAR grid points nearest to the glacier (Matulla et al., 2002), the generated daily mean temperatures show a correlation of 0.97, the daily precipitation sums a correlation of 0.7 with the measured values from Daxigou MS from 2004–2007. The temperature records were downscaled through a multiple linear regression, whereas the method of artifical neural networks (Sauter et al., 2009) appeared to be most suitable for precipitation downscaling.

Figure 6 shows that calculated values are in good agreement with the observations, with a correlation of 0.98 and an RMSE of 332 mm w.e. This good performance indicates that the enhanced DDM captures the controlling mechanisms of ablation and accumulation despite the short length of the calibration period.

Corresponding results for the simple temperature based DDM show a correlation of 0.74 and an RMSE of 21 mm w.e. for the calibration period (20–25 July 2007) as well as a correlation of 0.91 with an RMSE of 531 mm w.e. for the evaluation period (1987/88–2004/05), respectively.

Measured net mass balances in the years 2000/01–2002/03 are missing and therefore are not considered. The enhanced temperature-radiation DDM clearly underestimates the mean mass balances in the years 1988/89, 1989/90, 1991/92 and 1995/96, where measured net balance values were slightly positive (Fig. 7a and b). This is probably due to an overestimation of mean temperatures and an underestimation of precipitation amounts and thus accumulation rates within the reanalysis database. The large fraction of snow in the total precipitation amount leads to a positive feedback on glacier surface albedo and thereby on ablation rates especially in summer when shortwave radiation input is largest (Ageta and Higuchi, 1984). Until the balance year 1992/93 the model produces significantly less melt, except for the positive years mentioned above. This underestimation of melt is a result of disregarding a changing glacier area through the utilisation of a single glacier mask of the year 1999. This is illustrated in Fig. 8, where model results are compared to the net balance maps published by the WGMS. In former years a larger ablation area leads to more negative mass balance values than the model produces. Since the balance year 1992/93, the changing glacier area seems to have no distinct impact on the differences between measured and modelled mass balances.

In order to assess the improvement of the enhanced DDM on the spatial distribution of ablation and accumulation, the distributed mass balance obtained from the enhanced temperature-radiation DDM and the simple DDM, based only on air temperature are compared to the net balance maps published by the WGMS, respectively. The balance years 1992/93 to 1994/95 were exemplarily chosen, as the difference between measured and generated mass balance values are minimal. In the year 1999/2000 the glacier mask used in the model matches the glacier area of the balance map best (Fig. 8). Due to the resolution of the DEM of 28.5 m, the shape of the mask is dependent on the grid cells and therefore not perfectly fitting to the real glacier area.

The WGMS balance maps result from the spatial interpolation of the stake measurements solely. Thus, their accuracy highly depends on the density of the observing network (WGMS, 2007). Under consideration of the stake network, illustrated in Fig. 1 for the year 2007, it is obvious that the radiation induced complexity of the mass balance distribution cannot be captured sufficiently. Several structures, such as the upward shift of the isolines in the western parts of UG1 are reproduced better applying the enhanced DDM. In these areas the stake network is denser than in the eastern parts of the glacier. Therefore, it is possible to detect spatially varying melt rate patterns through mass balance measurements. In the western and southern parts of UG1, no ablation stake measurements can be considered for the balance maps. The interpolation is based on a temperature gradient explaining the better performance of the simple DDM in these areas when compared to the mass balance maps generated from measurements (Fig. 8).

Both DDMs reproduce the spatial pattern of the absolute mass balance in the WGMS maps with only limited success. In general, ablation in the lower parts and accumulation in the upper regions, each are underestimated, causing overall smaller mass balance gradients. This could be the effect of an imprecise temperature lapse rate and neglect of any precipitation gradient. The modelled equilibrium lines are shifted upward compared to the measured ones, while still the enhanced DDM performs superior over the simple DDM in this respect. The accurate location of isolines in the eastern parts of the lower glacier tongue cannot be identified in both DDMs. However, with regard to the stake network, the accuracy of this pattern in the measured data is questionable as well.

7 Conclusions

The enhanced temperature-radiation-index model including incoming direct shortwave radiation performed well in reproducing the time series of mass balance of UG1 during the 18year period 1987/88–2004/05, despite its simplicity, the few input data needed and the insufficient length of the calibration period. In positive mass balance years, melt is overestimated by the model, mostly due to an underestimation of precipitation amounts within the reanalysis data used as input.

The spatial distribution of annual mean surface mass balance in detail, as illustrated in the net balance maps (Fig. 8) is reproduced better applying the enhanced temperature-radiation-index model compared to the simple DDM. Including a term for shortwave radiation takes into account the effects of topography, which leads to higher melt rates in the western parts of the east branch of UG1. The equilibrium line altitudes, as well as the absolute values of lowest and highest melt rates, are closer to the measured values in this case.

In order to improve the model output and also in order to capture the positive balance years more adequately, a calibration period of extended length with daily mass balance measurements would be crucial. The continued operation of the AWS on the east branch of UG1 will allow for more reliable temperature and precipitation gradients in the future.

Acknowledgements. The staff of Tianshan Glaciological Station is gratefully acknowledged for their support during the whole campaign and especially during fieldwork. We thank the associated students for their help in collecting field data, Wang Feiteng, Chinese Academy of Sciences (CAS) for his scientific advice, Gunnar Ketzler, RWTH Aachen University for providing some of the instruments and Yang Huian, CAS for investigating and submitting the mass balance data from UG1 to WGMS. We also thank the staff from WGMS for their continuous work on collecting and providing glacier data. This work was supported by Tianshan Glaciological Station and the Department of Geography of RWTH Aachen University.

References

Ageta, Y. and Fujita, K.: Characteristics of mass balance of summer-accumulation type glaciers in the Himalayas and Tibetan Plateau, Z. Gletscherkd. Glazialgeol., 32, 61–65, 1996.

Ageta, Y. and Higuchi, K.: Estimation of mass balance components of a summer-accumulation type glacer in the Napal Himalaya, Geogr. Ann. A, 66(3), 249–255, 1984.

Braithwaite, R. J.: Calculation of degree-days for glacier-climate research, Z. Gletscherkd. Glazialgeol., 20, 1–8, 1984.
Braithwaite, R. J.: Positive degree-day factors for ablation on the Greenland ice sheet studied by energy-balance modelling, J. Glaciol., 41(137), 153–160, 1995.
Braithwaite, R. J. and Zhang, Y.: Sensitivity of mass balance of five Swiss glaciers to temperature changes assessed by tuning a degree-day model, J. Glaciol., 46(152), 4–14, 2000.
Domrös, M. and Peng, G.: The Climate of China. Springer-Verlag, Berlin, Heidelberg, New York, London, Paris, Tokyo, 1988.
Haeberli, W.: Glaciers and ice caps: historical background and strategies of world-wide monitoring, in: Mass balance of the cryosphere: Observations and modelling of contemporary and future changes, edited by: Bamber, J. L. and Payne, A. J., Cambridge University Press, Cambridge, 559–578, 2003.
Hagg, W.: Auswirkungen von Gletscherschwund auf die Wasserspende hochalpiner Gebiete, Vergleich Alpen – Zentralasien, Münchener Geogr. Abh., A53, 96 pp., 2003.
Hantel, M., Ehrendorfer, M., and Haslinger, A.: Climate sensitivity of snow cover duration in Austria, Int. J. Climatol., 20(6), 615–640, 2000.
Hock, R.: A distributed temperature-index ice- and snowmelt model including potential direct solar radiation, J. Glaciol., 45(149), 101–111, 1999.
Hock, R.: Temperature index melt modelling in mountain areas, J. Hydrol., 282, 104–115, 2003.
Jing, Z., Jiao, K., Yao, T., Wang, N., and Li, Z.: Mass balance and recession of Ürümqi glacier No. 1, Tien Shan, China, over the last 45 years, Ann. Glaciol., 43, 214–217, 2006.
Jóhannesson, T., Sigurdsson, O., Laumann, T., and Kennett, M.: Degree-day glacier mass-balance modelling with applications to glaciers in Iceland, Norway and Greenland, J. Glaciol., 41(138), 345–358, 1995.
Kalnay, E., Kanamitsu, M., Kistler, R., Collins, W., Deaven, D., Gandin, L., Iredell, M., Saha, S., White, G., Woollen, J., Zhu, Y., Chelliah, M., Ebisuzaki, W., Higgins, W., Janowiak, J., Mo, K. C., Ropelewski, C., Wang, J., Leetmaa, A., Reynolds, R., Jenne, R., and Joseph, D.: The NCEP/NCAR 40-Year Reanalysis-Project, B. Am. Meteorol. Soc., 77(3), 437–471, 1996.
Kumar, L., Skidmore, A. K., and Knowles, E.: Modelling topographic variation in solar radiation in a GIS environment, Int. J. Geogr. Inf. Sci., 11(5), 475–497, 1997.
Matulla, C., Penlap, E. K., and von Storch, H.: Empirisches downscaling – Überblick und zwei Beispiele, Beitrag für den Klimastatusbericht des DWD, 16 pp., 2002.

TCD
4, 207–232, 2010

Nelder, J. A. and Mead, R.: A simplex method for function minimization, Comput. J., 7, 308–313, 1965.
Oerlemans, J.: Glaciers and climate change, Swets & Zeitlinger BV, Lisse, Abingdon, Exton, Tokyo, 2001.
Ohmura, A.: Physical basis for the temperature-based melt-index method, J. Appl. Meteorol., 40, 753–761, 2001.
Pellicciotti, F., Brock, B., Strasser, U., Burlando, P., Funk, M., and Corripio, J.: An enhanced temperature-index glacier melt model including the shortwave radiation balance: development and testing for Haut Glacier d'Arolla, Switzerland, J. Glaciol., 51(175), 573–587, 2005.
Sauter, T., Schneider, C., Kilian, R., and Moritz, M.: Simulation and analysis of runoff from a partly glaciated meso-scale catchment area in Patagonia using an artificial neural network, Hydrol. Process., 23, 1019–1030, 2009.
Schuler, T. V., Hock, R., Jackson, M., Elvehoy, H., Braun, M., Brown, I., and Hagen, J. O.: Distributed mass-balance and climate sensitivity modelling of Engabreen, Norway, Ann. Glaciol., 42, 395–401, 2005.
Wang, N., Jing, Z., Jiao, K., Mikhalenko, V., Li, Z., Han, T., and Yang, H.: Variations of the Glacier No. 1 at the source of the Urumqi River, Tien Shan Mts., China, during the past 40 years, Data of Glaciol. Studies, 102, 48–53, 2007.
WGMS: Glacier Mass Balance Bulletin No. 3 (1992–1993), edited by: Haeberli, W., Hoelzle, M., and Bösch, H., IAHS (ICSI)/UNEP/UNESCO, World Glacier Monitoring Service, Zurich, 1994.
WGMS: Glacier Mass Balance Bulletin No. 4 (1994–1995), edited by: Haeberli, W., Hoelzle, M., and Suter, S., IAHS (ICSI)/UNEP/UNESCO, World Glacier Monitoring Service, Zurich, 1996.
WGMS: Glacier Mass Balance Bulletin No. 7 (2000–2001), edited by: Haeberli, W., Frauenfelder, R., Hoelzle, M., and Zemp, M., IAHS (ICSI)/UNEP/UNESCO/WMO, World Glacier Monitoring Service, Zurich, 2003.
WGMS: Glacier Mass Balance Bulletin No. 9 (2004–2005), edited by: Haeberli, W., Zemp, M., and Hoelzle, M., ICSU (FAGS)/IUGG (IACS)/UNEP/UNESCO/WMO, World Glacier Monitoring Service, Zurich, 2007.
Ye, B., Yang, D., Jiao, K., Han, T., Jin, Z., Yang, H., and Li, Z.: The Urumqi River source Glacier No. 1, Tianshan, China: Changes over the past 45 years, Geophys. Res. Lett., 32, 1–4, 2005.

Zhang, J. and Lin, Z.: Climate of China. John Wiley & Sons, Inc./Shanghai Scientific and Technical Publishers, New York, Chichester, Brisbane, Toronto, Singapore, Shanghai, 1992.
Zhang, Y., Liu, S., and Ding, Y.: Observed degree-day factors and their spatial variation on glaciers in western China, Ann. Glaciol., 43, 280–284, 2006a.
Zhang, Y., Liu, S., Xie, C., and Ding, Y.: Application of a degree-day model for the determination of contributions to glacier meltwater and runoff near Keqicar Baqiglacier, southwestern Tien Shan, Ann. Glaciol., 43, 280–284, 2006b.

Table 1. Adjusted parameters of the simple temperature index and the distributed temperature radiation model and their optimised values.

Parameter	Value
Temperature lapse rate[a]	$-0.71\,K\,(100\,m)^{-1}$
Precipitation gradient	0% $(100\,m)^{-1}$
Degree-day factor for ice, DDF_{ice} (simple DDM)	5.6 $(mm\,K^{-1}\,d^{-1})$
Degree-day factor for snow, DDF_{snow} (simple DDM)	2.8 $(mm\,K^{-1}\,d^{-1})$
Modified degree-day factor for ice, DDF^*_{ice} (enhanced DDM)	2.7 $(mm\,K^{-1}\,d^{-1})$
Modified degree-day factor for snow, DDF^*_{snow} (enhanced DDM)	1.35 $(mm\,K^{-1}\,d^{-1})$
Radiation factor a	14.7 (–)
Radiation factor b	8.8 (–)

[a] Derived from measurements.

TCD
4, 207–232, 2010

Title Page
Abstract Introduction
Conclusions References
Tables Figures
◂ ▸
Back Close
Full Screen / Esc
Printer-friendly Version
Interactive Discussion

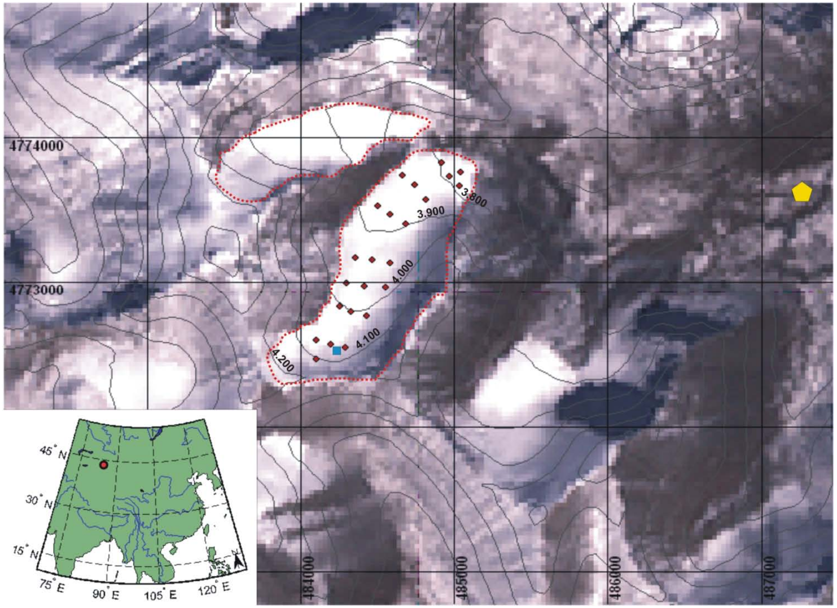

Fig. 1. Landsat TM image of the surrounding of Urumqi Glacier No. 1 in northwestern China. The glacier outlines are indicated by stippled lines. The dot in the outline map indicates the location of the glacier in Central Asia. The polygon marks the position of Daxigou Meteorological Station; the square indicates the position of the AWS on the east branch of UG1, the dots on the glacier mark the ablation stake network. Grid zone is UTM 45° N.

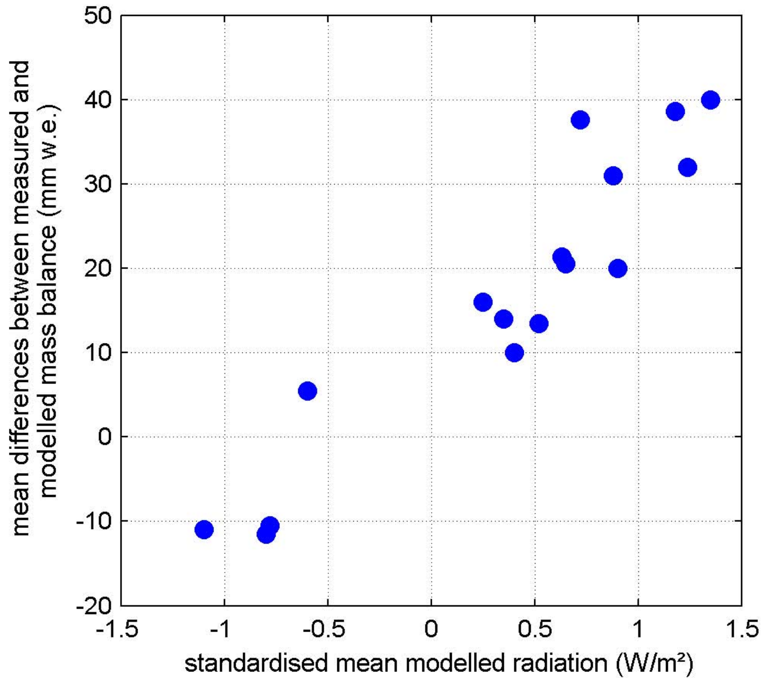

Fig. 2. Scatter plot of standardised mean modelled incoming radiation versus mean differences between measured and modelled mass balance for every ablation stake on UG1, mean values over six days (20 to 25 July 2007).

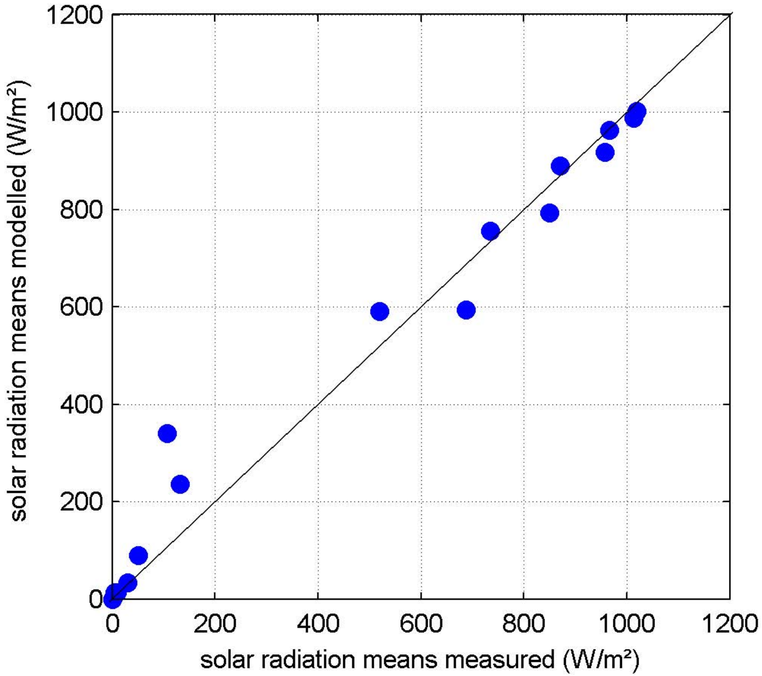

Fig. 3. Scatter plot of measured versus calculated mean hourly incoming shortwave radiation for the grid cell of the AWS on UG1 on 20 July 2007.

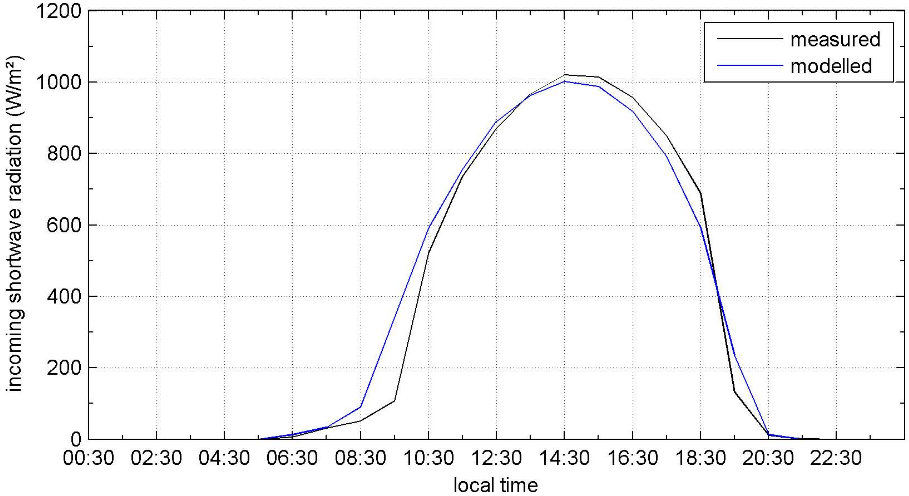

Fig. 4. Measured and modelled diurnal cycle of incoming shortwave radiation for the grid cell of the AWS on UG1 on 20 July 2007.

TCD

4, 207–232, 2010

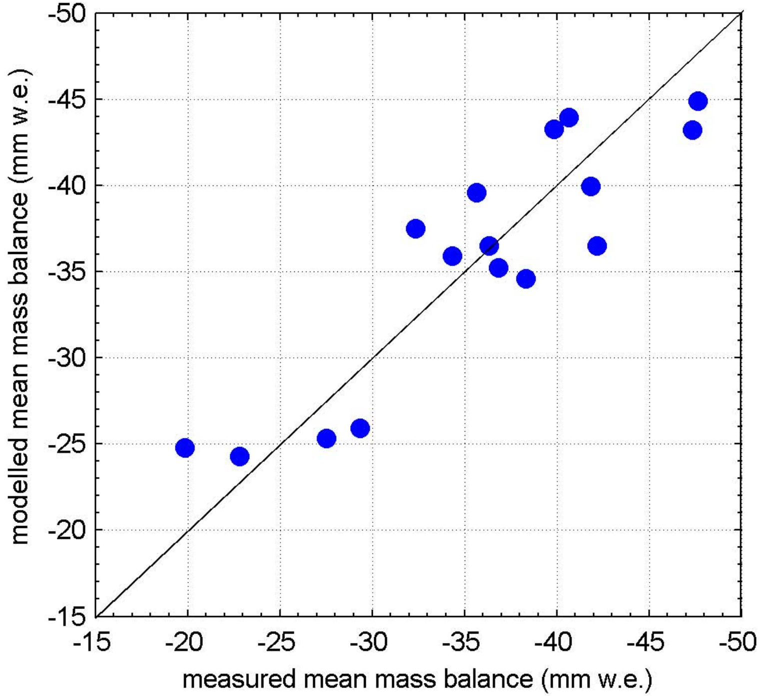

Fig. 5. Scatter plot of measured versus calculated mass balance at individual stakes on the east branch of UG1 (enhanced DDM); mean values over six days (20 to 25 July 2007). The number of samples is 102.

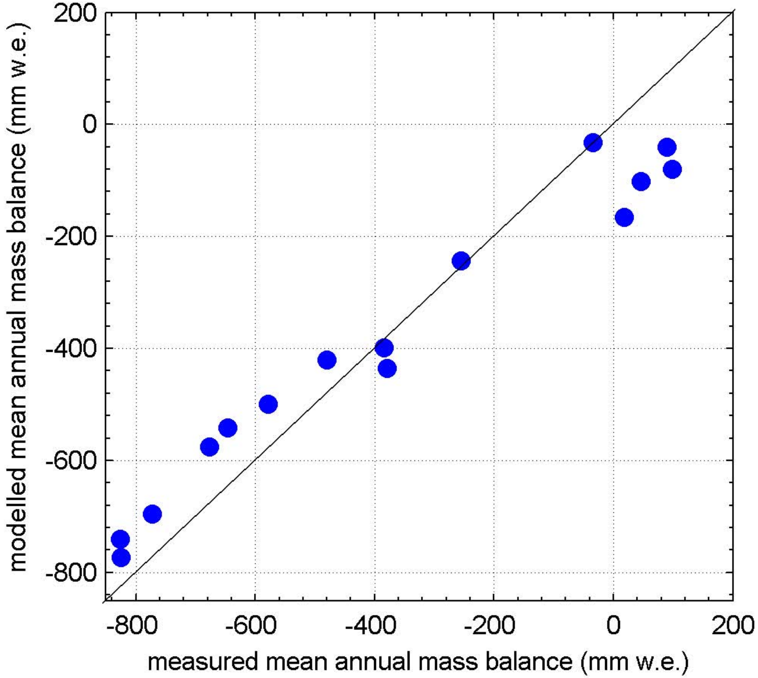

Fig. 6. Scatter plot of measured versus calculated mean annual mass balance of the east branch of UG1 (enhanced DDM), 1987/88–2004/05.

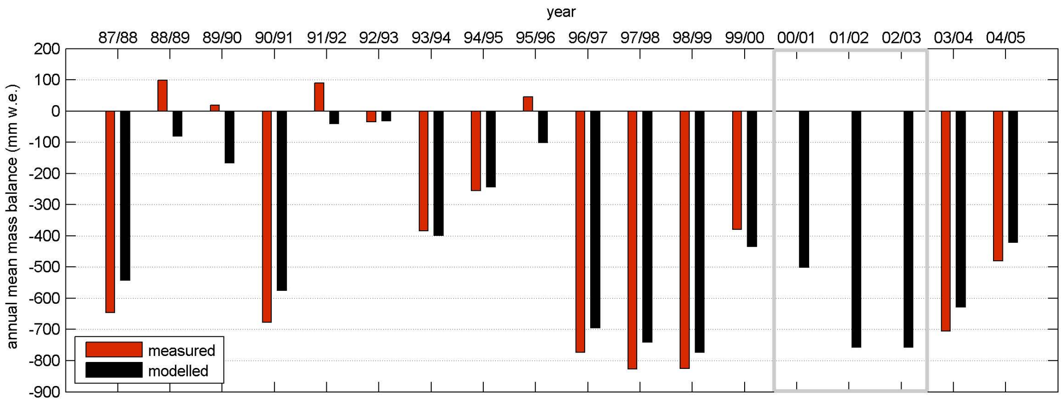

Fig. 7a. Mean values of annual mass balance of the east branch of UG1 (enhanced DDM), 1987/88–2004/05; for the period indicated by the grey border no mass balance measurements are available.

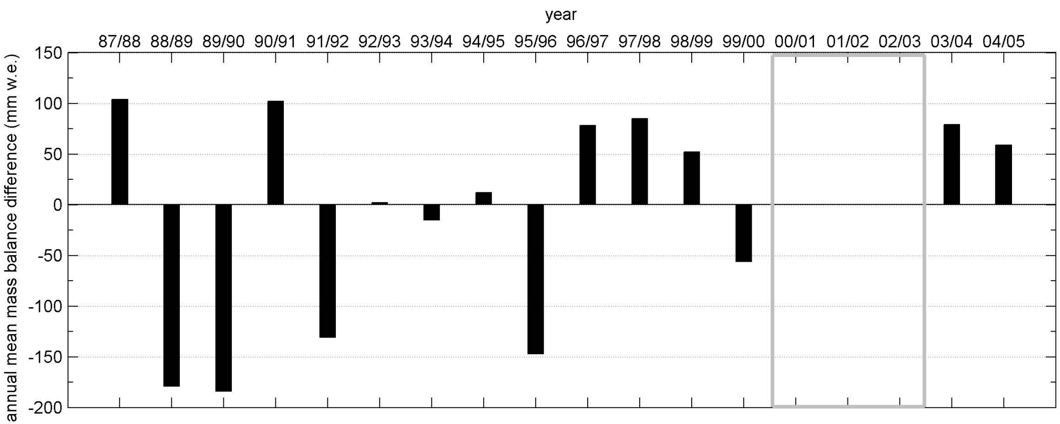

Fig. 7b. Annual mean differences between measured and modelled mass balance of the east branch of UG1 (enhanced DDM), 1987/88–2004/05, for the period indicated by the grey border no mass balance measurements are available.

TCD

4, 207–232, 2010

Degree-day modelling of the surface mass balance, Tian Shan

E. Huintjes et al.

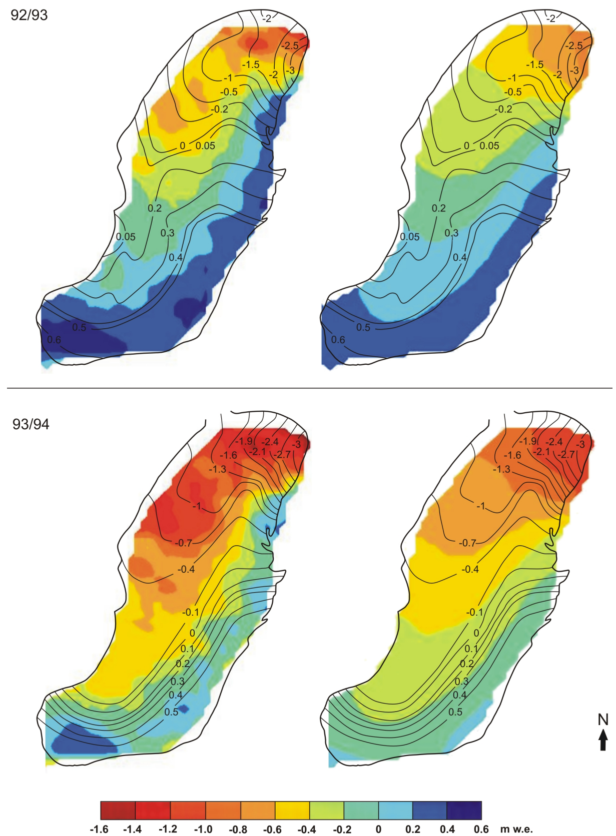

Fig. 8a. Comparison of modelled melt patterns and net balance maps published by WGMS for the years 1992/93, 1993/94, 1994/95 and 1999/2000. Left column: enhanced temperature-radiaton DDM, right column: simple merely temperature based DDM (WGMS 1994, 68, WGMS 1996, 73/74, WGMS 2003, 71).

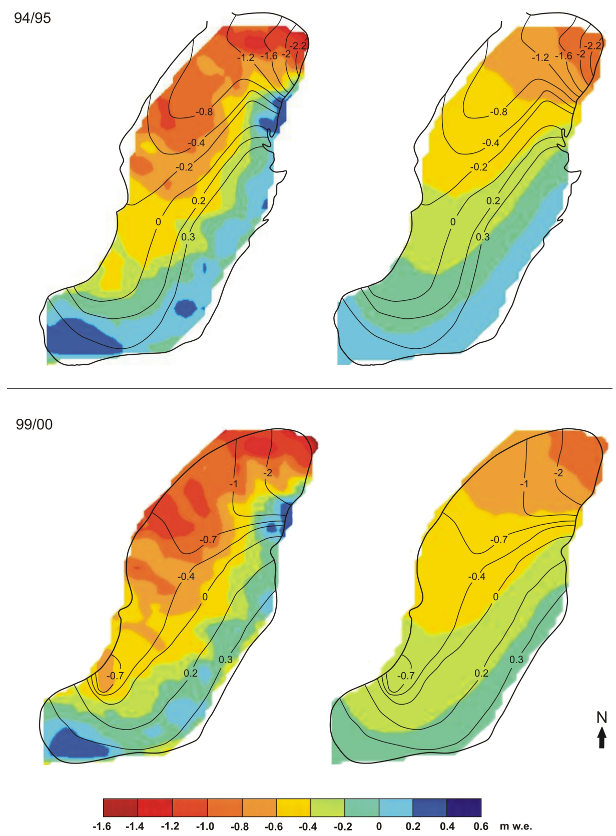

Fig. 8b.